# Skeletogenesis in Persian sturgeon (*Acipenser persicus*, Borodin, 1897) and its correlation with the gene expression of vitamin K dependent proteins along larval development

H. ESHAGHZADEH[1*], A. AKBARZADEH[1], M. YARMOHAMMADI[2] AND E. GISBERT[3]

[1] Department of Fisheries, Faculty of Marine Science and technology, University of Hormozgan, P.O. Box: 3995 Bandar Abbas, Iran, [2] International Sturgeon Research Institute, Agricultural Research, Education and Extension Organization (AREEO), P.O.Box:41635-3464, Rasht, Iran, [3] IRTA (Institut de Recerca i Tecnologia Agroalimentàries), IRTA-SRC, Unitat de Cultius Aqüícoles, Sant Carles de la Ràpita, Spain

[*]Corresponding author: Arash Akbarzadeh, Department of Fisheries, Faculty of Marine Science and technology, University of Hormozgan, P.O. Box: 3995 Bandar Abbas, Iran

Tel: +98 9170070375 Email: akbarzadeh@ut.ac.ir

**Running title: Skeletogenesis in *Acipenser persicus***

## ABSTRACT

The present study describes morphological development of the skeleton in the Persian sturgeon *Acipenser persicus* Borodin 1897, and discusses the hhypothesis that genes encoding vitamin k-dependant proteins (VKDPs) might have a correlation with the mineralization of skeletal tissues during early development in sturgeons. Results showed that the development of cartilage started just after hatching (10·9 ± 0·7 mm in total length, $L_T$) in the head and notochord, whereas the first signs of mineralization occurred in the dentary and in the dermopalatine and palatopterygoid elements of the upper jaw, coinciding with the onset of exogenous feeding (20·1 ± 1·5 mm $L_T$). All branchial arch elements were developed between 19·3 and 22·3 mm $L_T$, whereas mineralization was only observed in tooth plates associated with the hypobranchial 1 and gill rakers at 20·8 ± 1·5 mm $L_T$ and 48·4 ± 6·4 mm $L_T$, respectively. Quantitative real-time PCR showed that transcripts of VKDP genes including bone Gla protein (*bgp*), matrix Gla protein (*mgp*) and Gla rich protein (*grp*) were significantly up-regulated during the transition to exogenous feeding, supporting hypotheses about relevance of the above-mentioned genes in chondrogenesis at early deverlopmental stages. The strong mineralization of skeletal elements from 21·5 – 27·3 mm $L_T$ (20 dph) was in accordance with the maximal levels of *bgp, mgp* and *grp* expression indicating a correlation between development of the skeleton and the expression of VKDP genes. This information may be considered as a reference for future studies evaluating the quality of larvae and the influence of rearing biotic and abiotic factors on skeletogenesis and the occurrence of skeletal deformities in this species.



Key words: development, gene expression, skeleton, vitamin k-dependant proteins.

## INTRODUCTION

The fish skeletal system provides mechanical support to soft tissues and levers for muscle action, providing greater efficiency for locomotion, among other functions such as the mobilization or deposition of calcium and phosphorus which contributes to calcium homeostasis (Boglione *et al.*, 2013a). Skeletogenesis is therefore important not only for understanding changes in swimming behaviour (Osse & Van den Boogart, 1995), but also for evaluating the quality of hatchery-produced fish (Boglione *et al.*, 2013a, b). Skeletal abnormalities mostly appear during larval and early juvenile stages, when the skeleton differentiates and achieves its definitive configuration (Boglione *et al.*, 2013a). Many factors such as physiological, environmental, genetic, xenobiotic and nutritional can affect this process (Boglione *et al.*, 2013b); therefore, analysis of the skeletal system at early stages of development is an useful tool for assessing rearing conditions (i.e. environmental and nutritional) and their quality, regardless of whether fish are to be used for stocking or food production. Skeletogenesis must also be understood to understand the expression of skeleton-associated genes and proteins (Gavaia *et al*., 2006; Fernández *et al*., 2011). The formation of bones and other cartilaginous and mineralized tissues in fishes depends upon the expression of a wide variety of genes (Boglione *et al*. 2013a). This study examines a particular group of genes coding for vitamin k-dependant proteins (VKDPs), also known as γ-carboxyglutamic acid (Gla) proteins, including bone Gla protein (BGP), matrix Gla protein (MGP) and Gla rich protein (GRP) (see review in Dourado-Villa *et al*., 2017).

These proteins belong to the family of $Ca^{2+}$-binding vitamin K-dependent proteins and are recognized by having several Gla residues that are converted from the post-translation modifications of specific glutamates (Glu) via the γ-glutamyl carboxylase enzyme (GGCX) (Vermeer, 1990; Viegas *et al*., 2008). Both BGP (osteocalcin) and MGP are important in the regulation of mineral deposition in calcified tissues (Hashimoto *et al*., 2001; Viegas *et al*., 2013). BGP is synthesized by osteoblasts and odontoblasts and functions as a regulator of bone maturation (Boskey *et al*., 1998; Krossøy *et al*., 2009). MGP is also synthesized by osteoblasts but, in contrast to BGP, it is also synthesized by a wide variety of other cells, like vascular smooth muscle cells and chondrocytes (Krossøy *et al*., 2009). MGP is believed to be more important for regulating mineral deposition in vascular system and cartilage and it has a minor role in the regulation of chondrocyte maturation (Luo *et al*., 1997). GRP may also directly influence mineral formation, thereby playing a role in processes involving connective tissue mineralization (Viegas *et al*., 2009). In the skeleton, most relevant levels of *grp* gene expression have been observed in cartilaginous tissues and associated with chondrocytes and chordoblasts (Viegas *et al*., 2009; Cancela *et al*., 2012), suggesting a role in chondrogenesis. However, *grp* expression has also been detected in bone cells, which is indicative of a more widespread role for the protein throughout skeletal formation (Cancela *et al*., 2012; Dourado-Villa *et al*., 2017). Previous studies in teleosts have revealed an increase in expression of both *bgp* and *mgp* genes, paralleling calcification of axial skeleton structures during larval development (Gavaia *et al*., 2006). Despite the potential role of VKDPs in soft tissue mineralization and bone formation, little is known about the expression of genes encoding VKDPs (*i.e. mgp, bgp* and *grp*)

during sturgeon larval development. However, it has been found that the expression of *bgp*, *mgp* and *grp* genes in cartilaginous and bony tissues occurs in higher levels in adult sturgeons compared to mammals (Viegas *et al*., 2008; Viegas *et al*., 2013) and teleosts (Krossøy *et al*., 2009).

Continuous drastic declines in natural sturgeon populations over the past 30 years plus a high market demand for caviar have led the way for sturgeon farming, mainly for the production of caviar. According to Bronzi *et al.* (2011), the caviar output from aquaculture was 260 t in 2012, a production that was estimated to increase up to 500–750 t within the next 10 years. Sturgeons belong to the order Acipenseriformes (infraclass Chondrostei) and can provide useful information about mechanisms involved in the evolution of vertebrates, especially teleost fishes (Viegas *et al.*, 2013). Acipenseriformes diverged from the lineage leading to teleosts during the Devonian Age of Fishes (~385 million years ago) (Near et al., 2012) and in contrast to teleosts, they have retained a dermal skeleton (Jollie, 1980; Grande & Hilton, 2006; Hilton *et al.*, 2011). As Leprévost & Sire (2014) reviewed, few morphological studies on the skeleton of Acipenseriformes are available, even though a renewed interest in sturgeon biology has recently been promoted by their commercial importance, uniqueness and almost universally endangered status (Findeis, 1997). This information is incomplete and fragmented in terms of species, and also in terms of age; in particular, out of the 25 living acipenserid species, the skeleton of only 13 species and a hybrid has been studied, and the axial skeleton is often not the main topic of such studies (Leprevost & Sire, 2014). Considering the unique properties of the skeleton in Acipenseriformes, including an internal cartilaginous skeleton, five rows of bony plates, ganoid scales on the body

surface, and lack of a vertebral centrum (Viegas *et al*., 2008; Viegas *et al*., 2010), coupled with their distinctive skeletogenesis, it is worth investigating normal patterns of skeletal development, which will be essential to accurately assess deformities in hatchery-produced fry, detect critical stages during skeletogenesis and improve actual larval rearing practices in this commercially important and endangered group. Thus, the objectives of the present study were to describe the ontogenetic development of the skeleton of hatchery-reared Persian sturgeon (*Acipenser persicus* Borodin 1897), as well as to evaluate changes in the expression of genes encoding for VKDPs including *bgp*, *mgp* and *grp*, which are known to be involved in the formation and mineralization of skeletal tissue.

## MATERIAL AND METHODS

### *ANIMALS AND SAMPLING PROTOCOL*

Specimens of *A. persicus* were obtained from broodstock held at the Shahid Beheshti Artificial Sturgeon Propagation and Rearing Center (Rasht, Iran). Six adult individuals (two males and four females) were induced to spawn and spermiate with an intramuscular injection of LHRH-A2 hormone (3 μg $kg^{-1}$ body weight). Egg adhesiveness was removed by a 45-min treatment with a clay-water suspension; fertilised eggs were transferred to 15-L Yoshchenko incubators (500 g eggs per incubator) connected to an open-flow freshwater system. During the egg incubation period, water temperature was 14·4 ºC and progressively increased up to 17·4 ºC;

prelarvae hatched seven days after fertilization. At hatching, prelarvae were transferred to three 500-L circular fiberglass tanks with water depth of 30 cm, and initial density of 10 larvae $L^{-1}$ (10 g prelarvae per tank). *Artemia* nauplii were administered to larvae from eight days post hatching (dph) (150·2 degree days post hatching, ddph) to 12 dph (237·2 ddph) five times per day; after which larvae were fed with a mixture of cladocerans (*Daphnia* sp.) and *Artemia* metanauplii from 12 to 50 dph. Samples were taken at 10 different times: at hatching (0), 1, 3, 6, 10, 12, 14, 20, 30 and 50 dph. Fish were euthanized by an overdose of tricaine methanesulfonate (MS-222, Argent, Chemistry Laboratories, Redmond, USA), with 10 individuals immediately deep-frozen in liquid nitrogen and stored at −80 °C until RNA extraction. Ten additional individuals from the above-mentioned time-points were also fixed in 4% buffered formalin for descriptive purposes.

During fish rearing, water temperature, dissolved oxygen and pH levels were 14·2 ± 0·9 ºC, 7·9 ± 1·2 mg $l^{-1}$ and 7·4 ± 0·5, respectively. Photoperiod was 12L: 12D, and light intensity 200 lux at the water surface. Before fixation, the left side of each specimen was photographed using a Cannon camera (EOS 20D, 8 MP resolution) coupled to a stereomicroscope (EP600, Nikon, Japan), and total length ($L_T$) measured to the nearest mm using ImageJ (version 1·240). Yolk sac volume was determined according to Eshaghzadeh *et al.* (2017). Developmental stages of *A. persicus* were designated as prelarva, larva and early juvenile according to Dettlaff *et al.* (1993). The experimental work and fish procedures were carried out according to the requirements of The Iranian Society for The Prevention of Cruelty to Animals.

159 *STAINING OF THE SKELETON*

160 In order to describe the process of skeletogenesis in *A. persicus*, fish were stained
161 according to Hanken & Wassersug (1981). Briefly, samples were transferred into 100%
162 ethanol, rehydrated in gradually decreasing ethanol series (75, 50, and 25 %), and
163 washed with distilled water. Fish were incubated in Alcian blue (AB) solution (10 mg
164 Alcian blue 8GX, SIGMA A5268 in 70 ml absolute alcohol and 30 ml acetic acid).
165 Larvae were then incubated in a trypsin solution (1 g trypsin in 30% saturated borax
166 solution dissolved in 70 ml distilled water) for 2-8 hours depending on fish size. For
167 mineralized elements staining, specimens were transferred into a staining solution
168 containing 0·5% KOH and Alizarin red S (SIGMA T4799). Finally, fish were washed
169 with distilled water and then incubated in the gradually increasing series of glycerol +
170 1% KOH (25%, 50%, 75%, and pure glycerol) for clearing and complete elimination of
171 the nonspecific staining of soft tissues. Staining of cartilaginous skeletal structures by
172 Alcian blue solution at low pH values (pH = 2·0) did not result in important staining
173 skeletal artifacts [poor staining of mineralized elements, which are few in the skeleton of
174 Acipenseriformes (Hilton *et al.*, 2011; Leprevost & Sire, 2014)], since mineralized
175 elements were not decalcified during the cartilage staining step. Thus, the acid double
176 staining protocol used in this study (Hanken & Wasserug, 1981) was compared with the
177 acid-free staining protocol from Walker and Kimmel (2007) in early juveniles aged 50
178 dph (Figure 1).

179 *TOTAL RNA EXTRACTION AND COMPLEMENTARY DNA SYNTHESIS*

180 Total RNA was extracted from three separate individuals (biological replicates) using
181 Bioizol Reagent (Bioflux-Bioer, China) and treated with DNase I (Fermentas, France)

according to the manufacturer's instructions. The integrity of RNA was evaluated in a 1·5 % agarose electrophoresis gel and RNA quantity was determined by a NanoDrop ND-1000 Spectrophotometer (Thermo Scientific, Wilmington, DE, USA). All RNA samples had 260/280 ratios of 1·8-2·0 and 260/230 values of 2·0-2·2. One microgram of total RNA was used to synthesize first-strand cDNAs using a MMuLV reverse transcriptase and 2·5 μM oligo-dT following the manufacturer's instructions (Fermentas, France).

*PRIMER DESIGN AND QUANTITATIVE REAL-TIME PCR (qPCR)*

The qPCR primers for *bgp* and *grp* were designed based on sequences available in GenBank (accession numbers: EF413584, EU482149.1) from Adriatic sturgeon (*A. nacarii*) (Viegas *et al.*, 2008). Regarding *mgp*, primers were designed considering the sequence for *A. nacarii* (accession number: HM182000.1) and from two Teleostei species: turbot (*Scophthalmus maximus* (Linnaeus 1758)) and gilthead seabream (*Sparus aurata* (Linnaeus 1758)) (accession numbers: DQ304476.1, AY065652.1). qPCR primers were designed for each gene using Primer3 (Table 1) and the specificity and size of the amplicons obtained with primer pairs were checked on a 1·5% agarose gel. The fragments were sequenced using the ABI 3130 Genetic Analyzer (Applied Biosystems, USA). Chromatograms were checked and sequences manually aligned using the program BioEdit software Version 5. Identities of the sequences were verified by BLAST (http://ncbi.nlm.nih.gov/BLAST). Sequences obtained for *bgp*, *grp*, and *mgp* in *A. persicus* were submitted to GenBank (accession numbers: MF687668, MF687669 and MF687670, respectively). Primers for ribosomal protein L6 (*rpl6*) and β-actin

(*actb*), and their geometric average of messenger RNA (mRNA) level were used for the standardization of expression levels (Akbarzadeh *et al.*, 2011).

Quantitative real-time PCR (qRT-PCR) was run on a CFX96 Real-Time PCR Detection System (Bio-Rad, USA), using the CFX manager 1.6 software (Bio-Rad) and the following PCR protocol: pre-denaturation at 94 °C for 1 min, 40 cycles of denaturation at 94 °C for 15 s, annealing at 60 °C for 15 s, and extension at 72 °C for 30 s. Each reaction was performed using a total volume of 12 µl solution, with 1 x SYBR Green Bio-Easy mastermix (Bioer-Bioflux), 2·5 µM of ROX reference dye, 100 nM of each primer with 2 µl of cDNA template. Baseline, threshold (for Ct calculation), melting curve analysis (for verify the specificity of the target and absence of primer dimers) and standard curves (for PCR efficiency) among samples were determined as described in Akbarzadeh *et al*. (2011). Prior to statistical analysis, an amplification efficiency (E) was determined for each target gene as $E\% = (10^{1/slope} - 1) \times 100$, where the slope was estimated plotting the Ct in a serial dilutions of cDNA. Amplification efficiencies for all target and reference genes ranged between 91 to 99%. The mRNA expression of target genes (*bgp*, *mgp*, *grp*) relative to the reference genes (*actb* and *rpl6*) was calculated by the $2^{-\Delta\Delta Ct}$ method (Livak & Schmittgen, 2001). Among the developmental time-points, the sample at 1 dph was chosen as the reference sample to evaluate the differential mRNA expression of target genes.

*STATISTICS*

All qRT-PCR data were log-transformed and the homogeneity of variances and normality were assessed by Bartlett's and Kolmogorov–Smirnov tests, respectively.

Differences in gene expression data between different developmental time-points were analyzed by a one-way analysis of variance (ANOVA), followed by a Tukey's HSD *post hoc* analysis for multiple comparisons. Differences were considered statistically significant at $P < 0{\cdot}05$. SPSS (version 19·0) was used for statistical analysis.

## RESULTS

### *MORPHOLOGICAL DEVELOPMENT AND SKELETOGENESIS*

At hatching, prelarvae measured 10·9 ± 0·7 mm in $L_T$ and weighed 19·6 ± 0·3 mg in body weight (BW), showing a large yolk-sac (17·2 ± 4·4 $mm^3$). The posterior part of the body was surrounded by a wide primordial finfold, and no mineralized skeletal structures were visible (Figure 1a). Microscopic observations showed that sensory organs such as olfactory, gustatory and vision were not developed when prelarvae emerged from egg envelopes. At one dph (12·3 ± 0·9 mm $L_T$), the mouth and gill openings were cleaved with four branchial arches (AB-negative, but visible by transparency through the opercular region), pigmented eyes and barbel buds were also visible, and rudiments of the pectoral fin appeared like distinct folds. The head began to straighten and cartilaginous skeletal pieces started to stain with AB (Figure 1b). At three dph (14·1 ± 0·5 mm $L_T$), the finfold was wider on the ventral side of the trunk, narrowed at the caudal peduncle, and protruded slightly in the region where the future dorsal, caudal and anal fins will develop, the melanin plug (accumulation of melanin residues derived from yolk sac consumption) was visible in the anterior intestine, eyes were

250 darkly pigmented, the paired and single fins in the tail and trunk were still invisible.
251 Lower and upper lips were covered by small folds around the buccal cavity, and the
252 Meckel's and palatoquadrate cartilages appeared in the mandible and maxillary areas,
253 respectively (Figure 1c). At six dph (17·3 ± 0·8 mm $L_T$), the size of barbels increased
254 and the branchial cavity showed that external gills were not completely covered by the
255 operculum yet. Olfactory holes were joined to each other by olfactory lobes, yolk sac
256 was divided into two unequal parts and most of the yolk-sac was consumed, showing a
257 reduction in volume of about 76·2 % (Fig. 1d).

258 At 10 dph (19·9 ± 1·7 mm $L_T$), the dorsal fin was distinguishable from the
259 bordered margin of the posterior part of primordial finfold, teeth were already detected
260 in both jaws, but they were not mineralized (Figure 2a), and the rudiments of dorsal
261 scutes ($n$ = 9–11) were observed stained in Alcian blue in the dorsal part of the finfold.
262 Branchiostegals were clearly visible in the splanchnocranium, and gill arches were
263 completely formed. Several unmineralized structures, such as two basibranchial copulae,
264 three hypobranchials and five ceratobranchials were visible on the ventral portion of the
265 branchial arches at 10 dph (Figure 2d). Also, un-mineralized hyoid arches including the
266 hyomandybular, interhyal, hypohyal, and posterior and anterior ceratohyals were clearly
267 distinguished (results not shown). Cartilaginous elements of the subopercle, cleithrum
268 and postcleithrum appeared in the posterior margin of the head. In the hyoid arch, the
269 posterior end of the interhyal was linked to the ventral part of hyomandibular and
270 posterior ceratohyal, whereas the anterior end of the interhyal was connected to the
271 posterior portion of the lower jaw (palatoquadrate). At this age and body size, there still
272 seemed to be no mineralized elements in the skeleton of *A. persicus* (Figure 1e).

The first identified element to mineralize was the dentary, and also in the dermopalatine and palatopterygoid elements of the upper jaw at 12 dph (20·1 ± 1·5 mm $L_T$), coinciding with the onset of exogenous feeding. External gills were largely covered by the extended operculum, and teeth were observed arranged in a row on the dentary and dermopalatine mineralized elements, whereas two irregular rows of teeth were visible on the palatopterygoid mineralized element (Figure 2b). Between six and 12 dph, the formation of pelvic, anal and caudal fins was clearly distinguishable, whereas the dorsal fin had between 15 to 19 pterygiophores of the distal radials, middle radials and proximal radials, and five to seven metapterygial radials appeared in the pectoral fin. Unmineralized pterygiophores in the anal fin and between 22 to 26 unmineralized hypurals in the caudal fin were observed between 12 and 14 dph (20·8 ± 1·5 mm $L_T$). Hypurals developed on the anteriormost end of the caudal fin, forming its heterocercal structure (Figure 1f, g, j). No major changes in the formation of the skull were detected between 14 and 20 dph. Different mineralized skeletal elements from the cephalic region such as the subopercle, supracleithrum and parietal were found weakly mineralized at 20 dph (24·4 ± 2·9 mm $L_T$) (Figure 1h, 2c).

At 30 dph (33·4 ± 3·8 mm $L_T$), *A. persicus* specimens had a similar appearance to small juveniles and adults. At this age, the snout elongated and all morphological structures were totally developed and some new juvenile traits appeared such as five longitudinal rows of bony scutes, a ventrally-flattened body, elongated barbels, a completely differentiated heterocercal caudal fin composed of the basidorsals, basiventrals, distal radial, hypurals, supraneural and fin rays, and teeth on upper and lower jaw missing. Cartilaginous elements of the pelvic pterygiophores were observed at

30 dph (Figure 1i). Mineralization of the lateral row of scutes, cleithrum and rostral canal bones had already began at this age, while mineralization just started and continued to increase in the pectoral-fin spine, frontal, dermopterotic, jugal and dermosphenotic elements (Fig 1i). Finally, the last mineralized elements to form between 30 and 50 dph (48·4 ± 6·4 mm $L_T$; Fig 2e, f, g and 1j) were the parasphenoid, nasal, ventral and dorsal rostral elements, postorbital and median extrascapular bones, as well as two series of ventral scute rows ($n$ = 12–13 per row) where the posteriormost ventral scute of two scute series contact each other just after the anal fins. During this period, teeth on the mineralized dentary, dermopalatine and palatopterygoid elements disappeared.

*DEVELOPMENTAL EXPRESSION OF VKDPs CODING GENES*

Transcripts of *bgp*, *mgp* and *grp* were detected in all developmental time-points of *A. persicus* from one to 50 dph. Changes in *bgp* expression levels changed over development ($P < 0{\cdot}05$). As shown in Figure 3a, expression of *bgp* in *A. persicus* significantly increased from the onset of exogenous feeding at 10 dph to the early juvenile stage at 50 dph. The highest expression of *bgp* was observed at 30 dph when *A. persicus* resembled small juveniles.

Figure 3b illustrates changes in the expression levels of *mgp* during early development in *A. persicus*. Expression of *mgp* changed during prelarval, larval and early juvenile stages ($P < 0{\cdot}05$). Transcript levels of *mgp* followed a similar trend to that observed in *bgp* expression; specifically, *mgp* expression did not significantly vary

during the prelarval stage ($P > 0{\cdot}05$), whereas it significantly increased coinciding with the beginning of exogenous feeding and progressively increased until the early juvenile stage at 50 dph, although relative levels of *mgp* transcripts decreased at 30 dph ($P < 0{\cdot}05$), reaching similar values to those observed during the prelarval and larval stages, but increased again before the end of the study at 50 dph (Figure 3b).

Levels of *grp* transcripts showed a moderately increasing trend from one to 20 dph, except for 14 dph, although this trend was not statistically significant ($P > 0{\cdot}05$). At 30 dph the *grp* expression reached maximal value, whereas at 50 dph, *grp* values decreased and were similar to those observed at younger ages (one to six dph) (Figure 3c).

## DISCUSSION

Osteological studies are a very useful tool for understanding the functional demands and environmental needs of an organism during different stages of development (Boglione *et al.*, 2013a, b). According to the present study, the skeletal development of *A. persicus* could be divided into three main stages: 1) from hatching to the start of exogenous feeding (prelarval stage), during which cartilage elements of the skull with crucial roles in feeding and respiratory activity were formed but no mineralization occurred; 2) from the onset of exogenous feeding to the complete absorption of yolk sac reserves (mixed nutrition period), during which first mineralization processes and development of chondrogenesis related to feeding, swimming and respiratory activity occurred in larvae; and 3) from the end of the mixed nutrition period to the early juvenile period, which was

characterized by the development of all other mineralized elements of the skull roof (neurocranium), mineralization of bony scutes (dorsal, lateral and ventral in chronological order), appearance of the rostral sensory bone, and complete mineralization of cartilage elements that appeared at earlier stages.

The correct evaluation of mineralization is fundamental for the study of skeletal development maintenance, and regeneration (Bensimon-Brito *et al*., 2016). Some authors have reported that decalcification may occur in skeletal elements of teleost fish larvae, which are often only a few millimeters long, because of the use of acetic acid in the AB dye that may slightly demineralise skeletal elements and therefore lose their affinity for Alizarin red dye (Gavaia *et al*., 2000). Traditionally, cartilage is stained by AB blue using acidic conditions to differentiate tissue staining; however, the acidic conditions may be problematic when one wishes to stain the same specimen for mineralized bone with Alizarin red, because acid demineralizes bone by dissolving hydroxyapatite, which negatively affects bone staining (Walker & Kimmel, 2009). Data from this study with regard to the chronological development of small skeletal elements (*e.g.* dermopalatine, palatopterygoid, dentary, subopercle, supracleithrum, posttemporal and parietal) should be taken with caution since it is not possible to determine whether some demineralisation occurred in these elements due to the use of an acidic protocol double staining of skeletal structures (Walker & Kimmel, 2009). However, in the case of sturgeon larvae that are generally *ca*. five to 10 times larger than teleost larvae, we did not observe a remarkable loss of staining affinity to Alizarin red of skeletal elements, when using either acidic (Hanken & Wasserug, 1981) or non-acid (Walker and Kimmel, 2007) staining protocols, especially in dermal scute rows that were strongly stained in

red as soon as they were visible under the dissecting microscope. These differences between acipenserids and teleosts may be due to the larger size of sturgeon larvae in comparison to teleosts, as well as different staining-times employed between these fish groups. In this study, it took 30–60 min to stain sturgeon larvae of 10–24 mm, while for smaller marine teleost larvae (3-4 mm) at the same developmental stage staining time is shorter (10–15 min) (Gavaia *et al*., 2000).

*SKELETAL DEVELOPMENT*

According to the obtained results, no cartilaginous or mineralized elements were observed in the skull of *A. persicus* at hatching, whereas the notochord was the main skeletal element distinguishable at this stage. The lack of vertebral centra and the presence of a persistent notochord are considered as common features of the axial skeleton in the early ontogeny of sturgeons (Hilton *et al.*, 2011; Leprévost & Sire, 2014). The notochord is a medial structure that appears early in the embryo of all vertebrates, and has several important functions in biochemical and physiological signaling (Wang *et al*., 2014). In agreement with previous studies, the axial skeleton of *A. persicus* differs from that of teleost species. It is composed of a notochord, basidorsals, basiventrals, interdorsals, interventrals, neural spines, and ribs as in other sturgeon species (Hilton *et al.,* 2011; Zhang *et al.*, 2012; Leprévost & Sire, 2014). In *A. persicus*, the first mineralized bones, the dermopalatine, palatopterygoid and dentary were observed between 18·6–21·6 mm $L_T$ (12 dph). Mineralization of teeth and the complete covering of the external gills by the operculum, which might enhance prey seizure and gill development, respectively (Gisbert, 1999; Park *et al.,* 2013; Eshaghzadeh *et al*., 2017), are considered to be the most important events in the

development of the larval sturgeon splachnocranium, These changes were concomitant with the onset of exogenous feeding, the complete differentiation of the digestive organs and increase in digestive enzyme activities relative to earlier stages of development (Babaei *et al.,* 2011), which might be indicative of growth priorities during early development, which allometric growth studies have revealed in this group of fishes (Gisbert, 1999; Gisbert & Doroshov, 2006; Gisbert *et al*., 2014; Eshaghzadeh *et al*., 2017). In addition, the presence of unmineralized teeth and mineralized dentary and dermopalatine elements in *A. persicus* prelarvae just before the onset of exogenous feeding was in agreement with descriptions in shortnose sturgeon (*A. brevirostrum* Lesueur, 1818) (Hilton *et al*., 2011) and Siberian sturgeon (*A. baerii* Brandt, 1869) (Park *et al.*, 2013). Between 21·5 and 37·2 mm $L_T$ (20 and 30 dph), mineralization was observed in the following skeletal elements: the subopercle, supracleithrum, posttemporal, parietal and the dorsal scute row. These results are in contrast with those obtained in teleost fishes, which showed earlier mineralization in the above-mentioned cranial structures (Gluckmann *et al.*, 1999; Wagemans & Vandewalle, 2001). In this study, the initial formation of dorsal, lateral and ventral rudimentary scute rows took place asynchronously with regard to age and fell within the values reported for other acipenserid species. In particular, the initial formation and mineralization of dorsal scutes in *A. brevirostrum* were detected between 20·5 to 21·9 mm $L_T$ (Hilton *et al.*, 2011), whereas these occurred between 19.7 to 21.0 mm $L_T$ (Gisbert, 1999), and 20·6 to 26·0 mm $L_T$ (Park *et al.*, 2013) in *A. baerii*, although no specific methods using double-staining techniques were used for evaluating the development and mineralization of skeletal structures in either study of *A. baerii*. Similar to other sturgeon species, the

409 order of mineralization of scute rows in *A. persicus* began with the dorsal followed by
410 the lateral and then ended with the ventral row (Hilton *et al.*, 2011; Park *et al*., 2013;
411 Gisbert *et al*., 2014; Eshaghzadeh *et al*., 2017), although there existed some species-
412 specific variations in the sequence of scute formation and mineralization, which might
413 be related to many factors including different growth rates, availability of dietary
414 minerals, and different rearing conditions as has been postulated (Khajepour &
415 Hosseini, 2010; Park *et al.*, 2013).

416 The chronological order of formation of the neurocranial dermal skeleton in *A.*
417 *persicus* was characterized by initial development of the parietal mineralized elements
418 followed by the frontal and parasphenoid between 20 and 30 dph. Similary, in *A.*
419 *brevirostrum*, the first signs of mineralization in the neurocranium were observed in
420 both parietals (Hilton, 2005; Hilton *et al.*, 2011). Several structures of the
421 splanchnocranium, such as the Meckel's cartilage, pars autopalatina, hyoid arch,
422 dermopalatine and dentary, were differentiated just before the onset of exogenous
423 feeding in *A. persicus*, likely due to the important role they play in protractile-mouth-
424 type suction feeding behavior that is typical of sturgeons (Wagemans & Vandewalle,
425 2001). As Hilton *et al.* (2011) described, elements of upper and lower jaws are fused to
426 each other through the hyoid arches, and mandibular elements are not joined to the
427 neurocranium in sturgeon species. Moreover, the hyomandibular is inserted directly
428 between the neurocranium and opercular elements. In *A. persicus*, suspensorium
429 elements were developed simultaneously at 18·2–21·6 mm $L_T$ (10 dph), but no
430 mineralized elements were observed before the end of the study. However, in older
431 specimens of *A. brevirostrum*, some parts of the hyoid arch such as the hyomandibular,

the interhyal and the anterior ceratohyal were completely mineralized (Hilton, 2005; Hilton *et al.,* 2011). Mineralization of suspensorium elements developed gradually and jaw protrusion coincided with the loss of temporary teeth and a shift in the type of feeding from prey seizure to suction feeding by creating negative pressure in buccal cavity (Gisbert & Doroshov, 2003). Different mineralization patterns have been observed in the branchial arches of acanthopterygians (Wagemans & Vandewalle, 2001). In *A. persicus*, all of the branchial arch elements were completely developed between 19·3 and 22·3 mm $L_T$ (14 dph), whereas mineralization was only observed in teeth plates associated with hypobranchial 1 and gill rakers at 20·8 ± 1·5 mm $L_T$ (14 dph) and 48·4 ± 6.4 mm $L_T$ (50 dph), respectively. Differences in the time of mineralization in branchial arch elements are likely related to feeding type (suction feeding), the late transition from cutaneous to gill respiration in comparison to the teleost larvae, the increasing nutritional demands associated with suction feeding and the methodology used for bone and cartilage staining (Wagemans & Vandewalle, 2001; Boglione *et al*., 2013a).

After the development of mineralized and cartilage elements related to feeding and respiratory systems, which occurred between 19·9 ± 1·7 and 20·1 ± 1·5 mm $L_T$ (10 and 12 dph), the next priority in terms of osteological development in *A. persicus* larvae was the development of skeletal elements needed for supporting unpaired and paired fins. The first fins to form in chronological order were the pectoral fins, followed by the dorsal, anal and caudal fins, with pelvic fins being the last ones to form. Formation of the pectoral girdle was concomitant with the onset of exogenous feeding, which may be linked to the need for pectoral fins to assist with orienting the mouth over prey,

correcting head yaw (Osse *et al.*, 1995), promoting body roll, and affecting changes in vertical body position during maneuvering as described by Wilga & Lauder (1999). A similar sequence of fin formation was shown in bony fish (Sfakianakis *et al.*, 2004) and sturgeons (Hilton *et al.*, 2011).

*EXPRESSION OF VKDPs CODING GENES*

In the present study, the mRNA levels of genes encoding extracellular matrix proteins (*bgp*, *mgp* and *grp*) were up-regulated from 10 dph, at the time when *A. persicus* larvae started exogenous feeding. Regardless of the fact that these genes are not only expressed in skeletal structures (Dourado-Villa *et al*., 2017), the up-regulation of genes encoding *bgp*, *mgp* and *grp* in *A. persicus* was consistent with initial mineralization and chondrogenesis processes related to feeding, swimming and respiratory systems. These results suggest that bone and cartilage-related Gla proteins play a role in skeletal mineralization in sturgeons, if translation efficiency is not affected and translation occurred consistent with mRNA expression. The biological importance of the increasing trend in *mgp*, *bgp* and *grp* expression observed in this study could be related to the need for more efficient mechanisms to control mineralization, and development of organs and systems needed to meet the functional demands of the developing larvae (Gavaia *et al.*, 2006; Wang *et al.*, 2014). Comparison of the results obtained from this study and available data from higher vertebrates (Gavaia *et al.*, 2006; Viegas *et al.*, 2013), strengthen the hypothesis of a conserved function for Gla proteins from Acipenseriformes to humans, which span more than 450 million years of evolution.

The mRNA expression of *bgp* increased from the onset of exogenous feeding to the end of the study. The *bgp* protein is produced by osteoblasts in elements undergoing mineralization and odontoblasts during skeletogenesis (Pinto *et al.,* 2001). BGP has been shown to be a highly significant protein in bony tissues in amphibians (Viegas *et al.,* 2002), teleosts and sturgeon fishes (Bensimon-Brito *et al*., 2012; Viegas *et al.,* 2013). The observed up-regulation of *bgp* from 10 dph onwards coincided with the start of mineralization of dermal elements of the head and body surface during larval development of *A. persicus,* which could be attributed to the role of BGP in skeletogenesis. Increasing *bgp* mRNA expression in *A. persicus* is similar to that observed in European sea bass (*Dicentrachus labrax*) (Linnaeus, 1758) (Darias *et al.,* 2010), zebrafish (*Danio rerio*) (Hamilton, 1822) and Senegalese sole (*Solea senegalensis* Kaup, 1858) (Gavaia *et al.,* 2006). This study is the first to examine mRNA expression of the *mgp* gene during larval development of a Chondrostei species. The least *mgp* transcript was observed during the endogenous feeding period, after which *mgp* levels increased until 30 dph and then decreased at 50 dph, coinciding with transition to the early juvenile stage. It has been previously found that MGP in sturgeons is the most densely γ-carboxylated protein among known MGPs in vertebrates, with seven Gla residues. This protein is known as a key regulator of chondral and intramembranous ossification, and is a basic factor for differentiation and maturation of chondrocytes (Viegas *et al.,* 2013). Recent studies have demonstrated the presence of *mgp* transcripts in a wide variety of soft, cartilaginous and bony tissues in both sturgeons (Viegas *et al.,* 2013) and modern teleosts such as Atlantic salmon (*Salmo salar*) (Krossøy *et al.,* 2009) and turbot (*Scophtalmus maximus*) (Linnaeus, 1758)

(Roberto *et al.*, 2009). The considerable up-regulation of *mgp* transcripts from 20 dph onwards, and particularly at 30 dph, in *A. persicus* could be related to the strong mineralization of different dermal elements from the head and body surface, such as the subopercle, supracleithrum, parietal, bony scutes from dorsal and ventral rows and the anal, pelvic, dorsal and caudal fins and their respective pterygiophores. The increasing trend in *mgp* transcript levels has also been observed in teleosts such as *D. rerio, S. senegalensis* and *S. aurata*, where highest *mgp* expression levels were observed during larval developmental phases coinciding with first feeding, metamorphosis and the end of the larval stage, respectively (Gavaia *et al.*, 2006; Fernández et al., 2011). The present study also observed that *grp* mRNA levels increased during *A. persicus* development. GRP plays a critical role in processes involving connective tissue mineralization, with the highest number of Gla residues in all vertebrates; the Gla domain confer on these proteins their ability to bind of calcium ions (Viegas *et al.*, 2013). Moreover, *grp* is most highly expressed in cartilaginous tissues, especially mature and immature chondrocytes of vertebra and in the upper and lower jaws, as well as in the chordoblast layer of the notochord in sturgeons, which suggests a more widespread role for GRP throughout skeletal formation (Viegas *et al.*, 2008).

## CONCLUSIONS

Results of the present study showed that cartilage development in *A. persicus* started just after hatching in the head and notochord. Initial mineralization processes seemed to occur in the dentary, dermopalatine and palatopterygoid elements of the upper jaw,

coinciding with the onset of exogenous feeding. Genes encoding extracellular matrix proteins (*bgp, mgp* and *grp*) were up-regulated during the exogenous feeding phase. Strong mineralization of the skeletal elements occurring between 21·5 and 27·3 mm $L_T$ (20 dph) was in accordance with maximal levels of *bgp, mgp* and *grp* mRNA expression, suggesting that genes encoding vitamin k-dependant proteins might be correlated with mineralization of dermal tissues during sturgeon development. These observations provide a reference for future studies seeking to evaluate larval quality and the influence of biotic and abiotic rearing factors in the skeletogenesis of *A. persicus* and the occurrence of skeletal deformities.

**Acknowledgments**

The authors would like to thank Shahid Beheshti Artificial Sturgeon Propagation and Rearing Center for providing *A. persicus* samples, and Dr. R. Kazemi, Dr. Cerny and Mr. M. Parashkoh for their helpful comments. Funding was provided by the research deputy of University of Hormozgan (Iran).

**References**

Akbarzadeh, A., Farahmand, H., Mahjoubi, F., Nematollahi, M. A., Leskinen, P., Rytkönen, K. & Nikinmaa, M. (2011). The transcription of l-gulono-gamma-lactone oxidase, a key enzyme for biosynthesis of ascorbate, during development

543 of Persian sturgeon (*Acipenser persicus*). *Comparative Biochemistry and*
544 *Physiology B* **158**, 282-288. http://doi.org/10.1016/j.cbpb.2010.12.005

545 Babaei, S. S., Kenari, A. A., Nazari, R. & Gisbert, E. (2011). Developmental changes of
546 digestive enzymes in Persian sturgeon (*Acipenser persicus*) during larval
547 ontogeny. *Aquaculture* **318**, 138-144. doi: 10.1016/j.aquaculture.2011.04.032

548 Bensimon-Brito, A., Cardeira, J., Cancela, M. L., Huysseune, A. & Witten, P. E. (2012).
549 Distinct patterns of notochord mineralization in zebrafish coincide with the
550 localization of Osteocalcin isoform 1 during early vertebral centra formation.
551 *BMC Developmental Biology* **12**, 28. doi: 10.1186/1471-213X-12-28

552 Bensimon-Brito, A., Cardeira, J., Dionísio, G., Huysseune, A., Cancela, M. L. & Witten,
553 P. E. (2016). Revisiting in vivo staining with alizarin red S-a valuable approach
554 to analyse zebrafish skeletal mineralization during development and
555 regeneration. *BMC Developmental Biology* **16**, 2. doi: 10.1186/s12861-016-
556 0102-4

557 Boglione, C., Gavaia, P., Koumoundouros, G., Gisbert, E., Moren, M., Fontagné, S.,
558 Witten, P. E. (2013a). Skeletal anomalies in reared European fish larvae and
559 juveniles. Part 1: normal and anomalous skeletogenic processes. *Reviews in*
560 *Aquaculture* **5**, S99-S120. doi: 10.1111/raq.12015

561 Boglione, C., Gisbert, E., Gavaia, P., Witten, P. E., Moren, M., Fontagné, S. &
562 Koumoundouros, G. (2013b). Skeletal anomalies in reared European fish larvae
563 and juveniles. Part 2: main typologies, occurrences and causative factors.
564 *Reviews in Aquaculture* **5**, S121-S167. doi: 10.1111/raq.12016

565 Boskey, A., Gadaleta, S., Gundberg, C., Doty, S., Ducy, P. & Karsenty, G. (1998).
566 Fourier transform infrared microspectroscopic analysis of bones of osteocalcin-
567 deficient mice provides insight into the function of osteocalcin. *Bone* **23**, 187-
568 196. http://doi.org/10.1016/S8756-3282(98)00092-1

569 Bronzi, P., Rosenthal, H. & Gessner, J. (2011). Global sturgeon aquaculture production:
570 an overview. *Journal of Applied Ichthyology* **27**, 169-175. doi: 10.1111/j.1439-
571 0426.2011.01757.x

572 Cancela, M. L., Conceição, N. & Laizé, V. (2012). Gla-rich protein, a new player in
573 tissue calcification? *Advances in Nutrition* **3**, 174-181.
574 doi:10.3945/an.111.001685

575 Darias, M., Lan Chow Wing, O., Cahu, C., Zambonino-Infante, J. & Mazurais, D.
576 (2010). Double staining protocol for developing European sea bass
577 (*Dicentrarchus labrax*) larvae. *Journal of Applied Ichthyology* **26**, 280-285. doi:
578 10.1111/j.1439-0426.2010.01421.x

579 Dettlaff, T. A., Ginsburg, A. S. & Schmalhausen, O. I. (1993). Sturgeon fishes.
580 Developmental biology and aquaculture. Springer-Verlag, Berlin. pp. 300.

581 Dourado-Villa, J. K., Diaz, M. A. N., Pizziolo, V. R. & Martino, H. S. D. (2017). Effect
582 of vitamin K in bone metabolism and vascular calcification: a review of
583 mechanisms of action and evidences. *Critical Reviews in Food Science and*
584 *Nutrition*, in press. http://dx.doi.org/10.1080/10408398.2016.1211616

585 Eshaghzadeh, H., Alcaraz, C., Akbarzadeh, A. & Gisbert, E. (2017). The combination of
586 bivariate and multivariate methods to analyze character synchronization and
587 early allometric growth patterns in the stellate sturgeon (*Acipenser stellatus*
588 Pallas, 1771) as tools for better understanding larval behavior. *Canadian Journal*
589 *of Fisheries and Aquatic Sciences*, in press. doi: 10.1139/cjfas-2016-0288

590 Fernández, I., Darias M., Andree K B., Mazurais D., Zambonino-Infante J. L. & Gisbert
591 E. (2011). Coordinated gene expression during gilthead sea bream skeletogenesis
592 and its disruption by nutritional hypervitaminosis A. *BMC Developmental*
593 *Biology* **11**, 1-7. doi: 10.1186/1471-213X-11-7

594 Findeis, E. K. (1997). Osteology and phylogenetic interrelationships of sturgeons
595 (Acipenseridae). *Environmental Biology of Fishes* **48**, 73-126. doi:
596 10.1023/A:1007372832213

597 Gavaia, P. J., Sarasquete, C. & Cancela, M. L. (2000). Detection of mineralized
598 structures in early stages of development of marine Teleostei using a modified
599 alcian blue-alizarin red double staining technique for bone and cartilage.
600 *Biotechnic & Histochemistry* **75**, 79-84. doi:
601 http://dx.doi.org/10.3109/10520290009064151

602 Gavaia, P. J., Simes, D. C., Ortiz-Delgado, J., Viegas, C. S., Pinto, J. P., Kelsh, R. N.,
603 Sarasquete, M. C. & Cancela M. L. (2006). Osteocalcin and matrix Gla protein
604 in zebrafish (*Danio rerio*) and Senegal *S. senegalensis*: Comparative gene and
605 protein expression during larval development through adulthood. *Gene*
606 *Expression Patterns* **6**, 637-652. http://doi.org/10.1016/j.modgep.2005.11.010

607 Gisbert, E. (1999). Early development and allometric growth patterns in Siberian
608 sturgeon and their ecological significance. *Journal Fish Biology* **54**, 852-862.
609 doi: 10.1111/j.1095-8649.1999.tb0203

610 Gisbert, E. & Doroshov, S. I. (2003). Histology of the developing digestive system and
611 the effect of food deprivation in larval green sturgeon (*Acipenser medirostris*).
612 *Aquatic Living Resources* **16**, 77-89. https://doi.org/10.1016/S0990-7440
613 (03)00029-9

614 Gisbert, E. & Doroshov, S. I. (2006). Allometric growth in green sturgeon larvae.
615 *Journal of Applied Ichthyology* **22**, 202–207. doi: 10.1111/j.1439-
616 0426.2007.00952.x

617 Gisbert, E., Asgari, R., Rafiee, G., Agh, N., Eagderi, S., Eshaghzadeh, H. & Alcaraz, C.
618 (2014). Early development and allometric growth patterns of beluga *Huso huso*
619 (Linnaeus, 1758). *Journal of Applied Ichthyology* **30**, 1264-1272. doi:
620 10.1111/jai.12617

621 Gluckmann, I., Huriaux, F., Focant, B. & Vandewalle, P. (1999). Postembryonic
622 development of the cephalic skeleton in *Dicentrarchus labrax* (Pisces,
623 Perciformes, Serranidae). *Bulletin of Marine Science* **65**: 11-36.

624 Grande, L., & Hilton, E. J. (2006). An exquisitely preserved skeleton representing a
625 primitive sturgeon from the Upper Cretaceous Judith River Formation of
626 Montana (Acipenseriformes: Acipenseridae: n. gen. and sp). *Journal of*
627 *Paleontology* **80**, 1-39. http://dx.doi.org/10.1666/05032.1

628 Hanken, J. & Wassersug, R. (1981). The visible skeleton. *Functional Photography* **16**,
629 22-26.

630 Hilton, E. J. (2005). Observations on the skulls of sturgeons (Acipenseridae): Shared
631 similarities of *Pseudoscaphirhynchus kaufmanni* and juvenile specimens of
632 *Acipenser stellatus*. *Environmental Biology of Fishes* **72**, 135-144. doi:
633 10.1007/s10641-004-6578-y

634 Hilton, E. J., Grande, L. & Bemis, W. E. (2011). Skeletal anatomy of the shortnose
635 sturgeon, *Acipenser brevirostrum* Lesueur, 1818, and the systematics of
636 sturgeons (Acipenseriformes, Acipenseridae). *Fieldiana Life and Earth Sciences*
637 **3**, 1-168.

638 Jollie, M. (1980). Development of head and pectoral girdle skeleton and scales in
639 Acipenser. *Copeia* **1980**, 226-249.

640 Khajepour, F. & Hosseini, S. A. (2010). Mineral status of juvenile beluga (*Huso huso*)
641 fed citric acid supplemented diets. *World Applied Sciences Journal* **11**, 682-686.

642 Krossøy, C., Ørnsrud, R. & Wargelius, A. (2009). Differential gene expression of bgp
643 and mgp in trabecular and compact bone of Atlantic salmon (*Salmo salar* L.)
644 vertebrae. *Journal of Anatomy* **215**, 663-672. doi: 10.1111/j.1469-
645 7580.2009.01153.x

646 Leprévost, A. & Sire, J. Y. (2014). Architecture, mineralization and development of the
647 axial skeleton in Acipenseriformes, and occurrences of axial anomalies in rearing

conditions; can current knowledge in teleost fish help? *Journal of Applied Ichthyology* **30**, 767-776. doi: 10.1111/jai.12525

Livak, K. J. & Schmittgen, T. D. (2001). Analysis of Relative Gene Expression Data Using Real-Time Quantitative PCR and the 2-ΔΔCT method. *Methods* **25**, 402-408. https://doi.org/10.1006/meth.2001.1262

Luo G., Ducy P., McKee M. D., Pinero G. J., Loyer E., Behringer R. R. & Karsenty G. (1997). Spontaneous calcification of arteries and cartilage in mice lacking matrix GLA protein. *Nature* **386**, 78-81. doi:10.1038/386078a0Osse, J. & Van den Boogaart, J. (1995). Fish larvae, development, allometric growth, and the aquatic environment. *ICES Marine Science Symposia* **201**, 21–34.

Near, T. J., Eytan, R. I., Dornburg, A., Kuhn, K. L., Moore, J. A., Davis, M. P. & Smith, W. L. (2012). Resolution of ray-finned fish phylogeny and timing of diversification. *Proceedings of the National Academy of Sciences of the United States of America* **109**, 13698–13703. http://doi.org/10.1073/pnas.1206625109

Park, C., Lee, S. Y., Kim, D. S. & Nam, Y. K. (2013). Effects of incubation temperature on egg development, hatching and pigment plug evacuation in farmed Siberian sturgeon *Acipenser baerii*. *Fisheries and Aquatic Sciences* **16**, 25-34. doi: 10.5657/FAS.2013.0025

Pinto, J., Ohresser, M. & Cancela, M. (2001). Cloning of the bone Gla protein gene from the teleost fish (*Sparus aurata*). Evidence for overall conservation in gene organization and bone-specific expression from fish to man. *Gene* **270**, 77-91. http://doi.org/10.1016/S0378-1119(01)00426-7

Roberto, V. P., Cavaco, S., Viegas, C. S., Simes, D. C., Ortiz-Delgado, J. B., Sarasquete, M. C., Gavaia, P. J. & Cancela, M. L. (2009). Matrix Gla protein in turbot (*Scophthalmus maximus*): Gene expression analysis and identification of sites of protein accumulation. *Aquaculture* **294**, 202-211. http://doi.org/10.1016/j.aquaculture.2009.06.020

Sfakianakis, D., Koumoundouros, G., Divanach, P. & Kentouri, M. (2004). Osteological development of the vertebral column and of the fins in (*Pagellus erythrinus* L. 1758). Temperature effect on the developmental plasticity and morpho-anatomical abnormalities. *Aquaculture* **232**, 407-424.https://doi.org/10.1016/j.aquaculture.2003.08.014

Vermeer, C. (1990). Gamma-carboxyglutamate-containing proteins and the vitamin K-dependent carboxylase. *Biochemical Journal* **266**, 625-636.

Viegas, C., Pinto, J., Conceicao, N., Simes, D. & Cancela, M. (2002). Cloning and characterization of the cDNA and gene encoding *Xenopus laevis* osteocalcin. *Gene* **289**, 97-107. http://doi.org/10.1016/S0378-1119(02)00480-8

Viegas, C., S. Simes, D. C., Laizé, V., Williamson, M. K., Price, P. A. & Cancela, M. L. (2008). Gla-rich protein (GRP), a new vitamin K-dependent protein identified from sturgeon cartilage and highly conserved in vertebrates. *Journal of Biological Chemistry* **283**, 36655-36664. doi: 10.1074/jbc.M802761200

Viegas, C. S., Simes, D. C., Williamson, M. K., Cavaco, S., Laizé, V., Price, P. A. & Cancela, M. L. (2013). Sturgeon osteocalcin shares structural features with matrix Gla protein: evolutionary relationship and functional implications.

692 *Journal of Biological Chemistry* **288**, 27801-27811. doi:
693 10.1074/jbc.M113.450213

694 Wagemans, F. & Vandewalle, P. (2001). Development of the bony skull in common
695 sole: brief survey of morpho-functional aspects of ossification sequence. *Journal*
696 *of Fish Biology* **59**, 1350-1369. doi: 10.1111/j.1095-8649.2001.tb00197.x

697 Walker, M. B. & Kimmel, C. B. (2007). A two-color acid-free cartilage and bone stain
698 for zebrafish larvae. *Biotechnic & Histochemistry* **82**, 23-28.
699 http://dx.doi.org/10.1080/10520290701333558

700 Wang, S., Furmanek, T., Kryvi, H., Krossøy, C., Totland, G. K., Grotmol, S. &
701 Wargelius, A. (2014). Transcriptome sequencing of Atlantic salmon (*Salmo*
702 *salar* L.) notochord prior to development of the vertebrae provides clues to
703 regulation of positional fate, chordoblast lineage and mineralisation. *BMC*
704 *Genomics* **15**, 141. doi: 10.1186/1471-2164-15-141

705 Wilga, C. & Lauder, G. (1999). Locomotion in sturgeon: function of the pectoral fins.
706 *Journal of Experimental Biology* **202**, 2413-2432.

707 Zhang, X., Shimoda, K., Ura, K., Adachi, S. & Takagi Y. (2012). Developmental
708 structure of the vertebral column, fins, scutes and scales in bester sturgeon, a
709 hybrid of beluga *Huso huso* and sterlet *Acipenser ruthenus*. *Journal of Fish*
710 *Biology* **81**, 1985-2004. doi: 10.1111/j.1095-8649.2012.03451.x

711

712 Table1. Candidate reference and target genes tested for quantitative real-time PCR in

713 *Acipenser persicus*.

| Genes | Primers, Forward/Reverse | Amplicon size |
|---|---|---|
| Bone Gla protein | F- TCTGACGCTGTTTTGCTCCAGTAAATCTCG | 95 |
| | R- CGTTTCAGGGAAAATACCCAAAAGCAATA | |
| Matrix Gla protein | F- CTGGCTACTACTATGAGAGGTTAATGG | 135 |
| | R- GGTCACATGGGGTGTGCT | |
| Gla Rich protein | F- TGTAGAGGAGGAGCGTGATGAGCAGCA | 163 |
| | R- CATGATGTCCTTTTTTGGCGATTGTGTTC | |
| beta-actin | F- TGGAGGTACCACCATGTACCC | 167 |
| | R- CACATCTGCTGGAAGGTGGA | |
| Ribosomal protein L6 | F- GTGGTCAAACTCCGCAAGA | 149 |
| | R- GCCAGTAAGGAGGATGAGGA | |

714

715

## Figure captions

**Fig. 1.** Skeletogenesis of *Acipenser persicus* from hatching (10·9 mm $L_T$) to 50 days post hatching (dph) (48·4 mm $L_T$). a) Hatching time, b) 1 dph, c) 3 dph, d) 6 dph, e) 10 dph, f) 12 dph, g) 14 dph, h) 20 dph, i) 30 dph, j) 50 dph (acidic staining) and k) 50 dph (non-acidic staining). *Abbreviations*: a= anus, br = branchiostegal, cha = anterior ceratohyal, chp = posterior ceratohyal, cl = cleithrum, clv = clavicle, dpt = dermopterotic, dr = distal radial, ds = dorsal scute, dsp = dermosphenotic, h= hyoid arch, hyp = hypural, ihy = interhyal, j = jugal, lrb = lateral rostral canal bone, m = melanin plug, mc = Meckel's cartilage, mr = middle radial, n = notochord, pa= palatoquadrates, pas = parasphenoid, pat = pars autopalatina, pf = primordial finfold, phy= parhypural, po = postorbital, pp = pelvic pterygiophore, pr= proximal radial, pt = posttemporal, rcb = rostral canal bones, scl = supracleithrum, so = supraorbital, sp= spiral valve (scale bar = 1 mm).

**Fig. 2.** Ventral and dorsal views of the head of *Acipenser persicus* showing the mineralization of different skeletal elements during larval development [19·9 - 48·5 mm $L_T$, 10 days post hatching (dph) to 50 dph]. a) Unmineralized teeth in both jaws at 10 dph; b) ventral view of the jaw at early stages of development (12 dph); c) weak mineralized dermal bones of head and dorsal scutes at 20 dph; d) ventral view of branchial arch at 10 dph, e) Strong mineraliztion of dermal bones in dorsal view of head; f & g) ventral view of hyoid arch at 50dph. *Abbreviations*: bbc = basibranchial copulae, cb = ceratobranchial, cha = anterior ceratohyal, chp = posterior ceratohyal, d = dentary,

738 dpl = dermopalatin, dpt = dermopterotic, drb = dorsal rostral bone, dsp =
739 dermosphenotic, excm = median extrascapular, fr = frontal, h = hyomandybula, hb =
740 hypobranchial, hh = hypohyal, ihy = interhyal, j = jugal, lrb = lateral rostral canal bone,
741 pa = parietal, pt = posttemporal, rcb = rostral canal bones, scl = supracleithrum, sop =
742 subopercle, t = teeth, vrb = ventral rostral bone (scale bar 1mm).

743

744 **Fig. 3.** $Log_2$ expression of the (a) *bgp*, (b) *mgp* and (c) *grp* genes during the
745 development of *Acipenser persicus* from 1 day post hatching (dph) to 50 dph. The
746 values are considered as mean ± SD (n = 3). Statistical significance of differences of the
747 normalized *bgp*, *mgp* and *grp* data between samples taken at different developmental
748 times was analyzed using one-way ANOVA followed by Tukey's multiple-comparison
749 test. Bars with different letters are significantly different ($P < 0{\cdot}05$).

750

751

752

753 Figure 1.

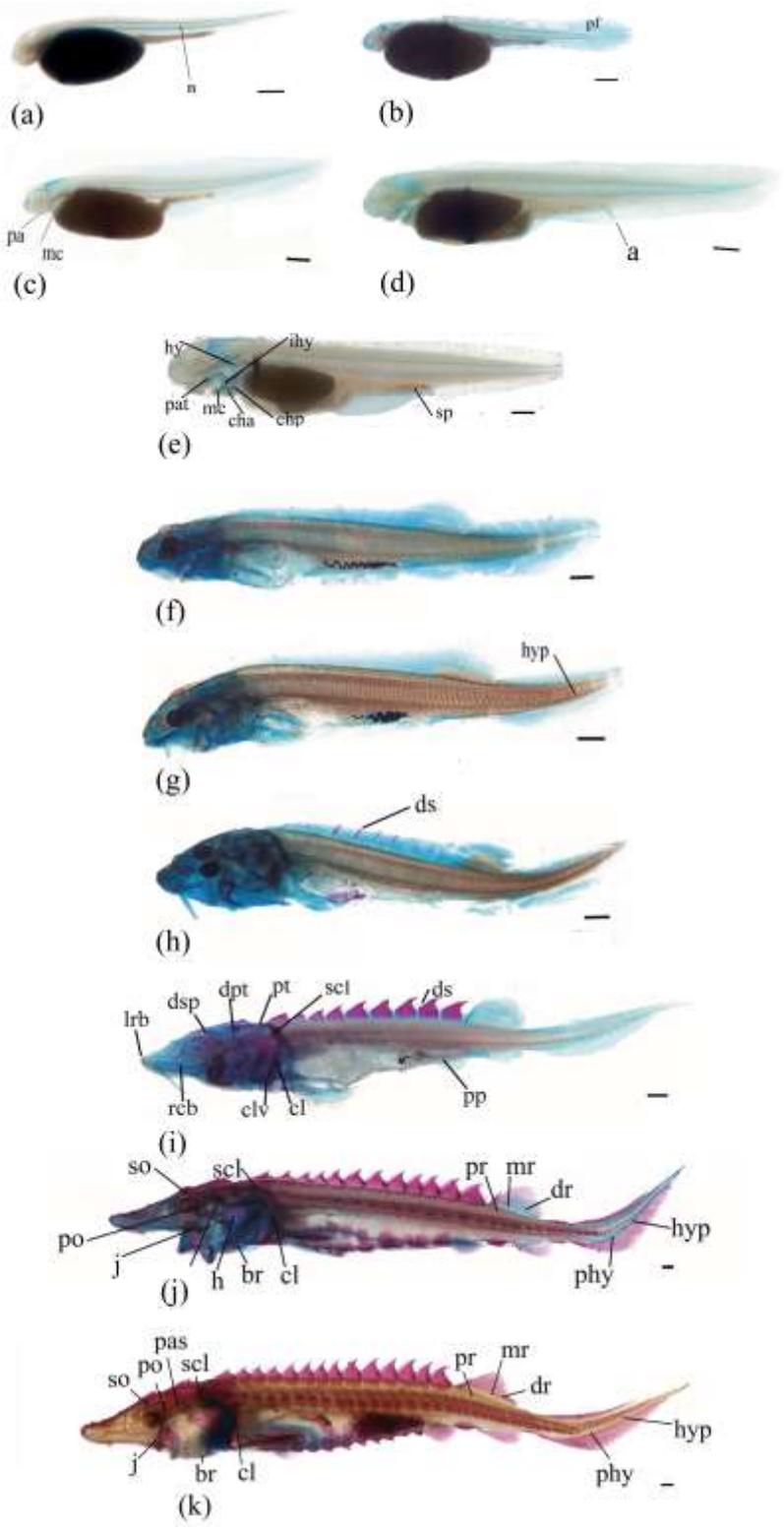


754

Figure 2

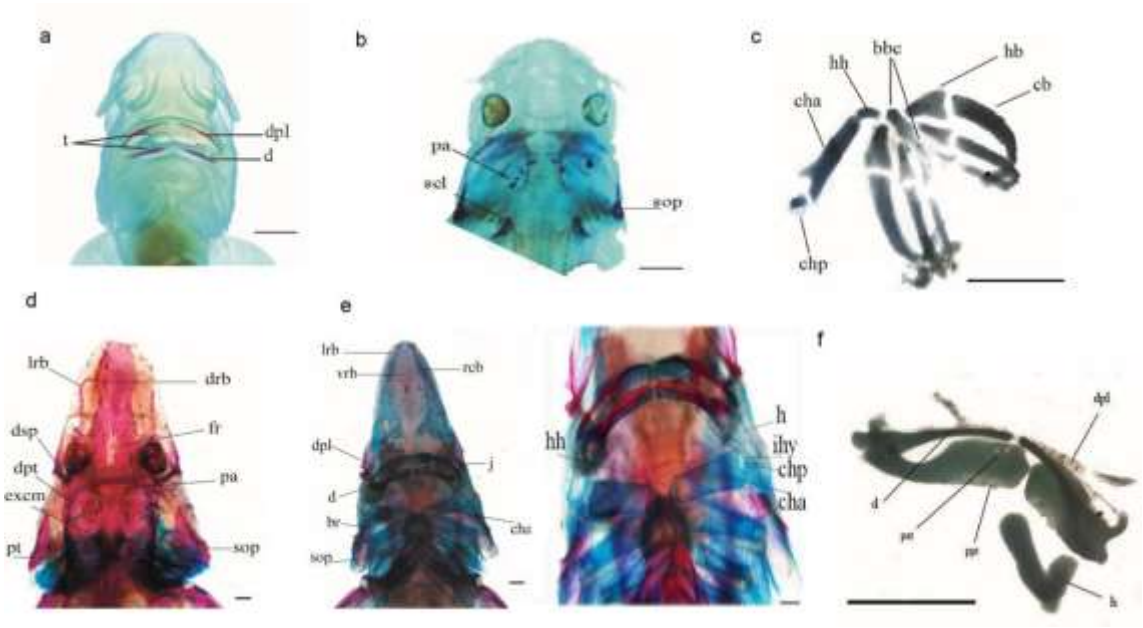
a
t
dpl
d
b
pa
scl
eop
c
bbc
hh
hb
cb
cha
chp
d
lrb
drb
dsp
fr
dpt
pa
excm
pt
sop
e
lrb
vrb
rcb
dpl
j
d
hc
cha
sop
hh
h
ihy
chp
cha
f
dpl
d
pa
pa
h

759 Figure 3

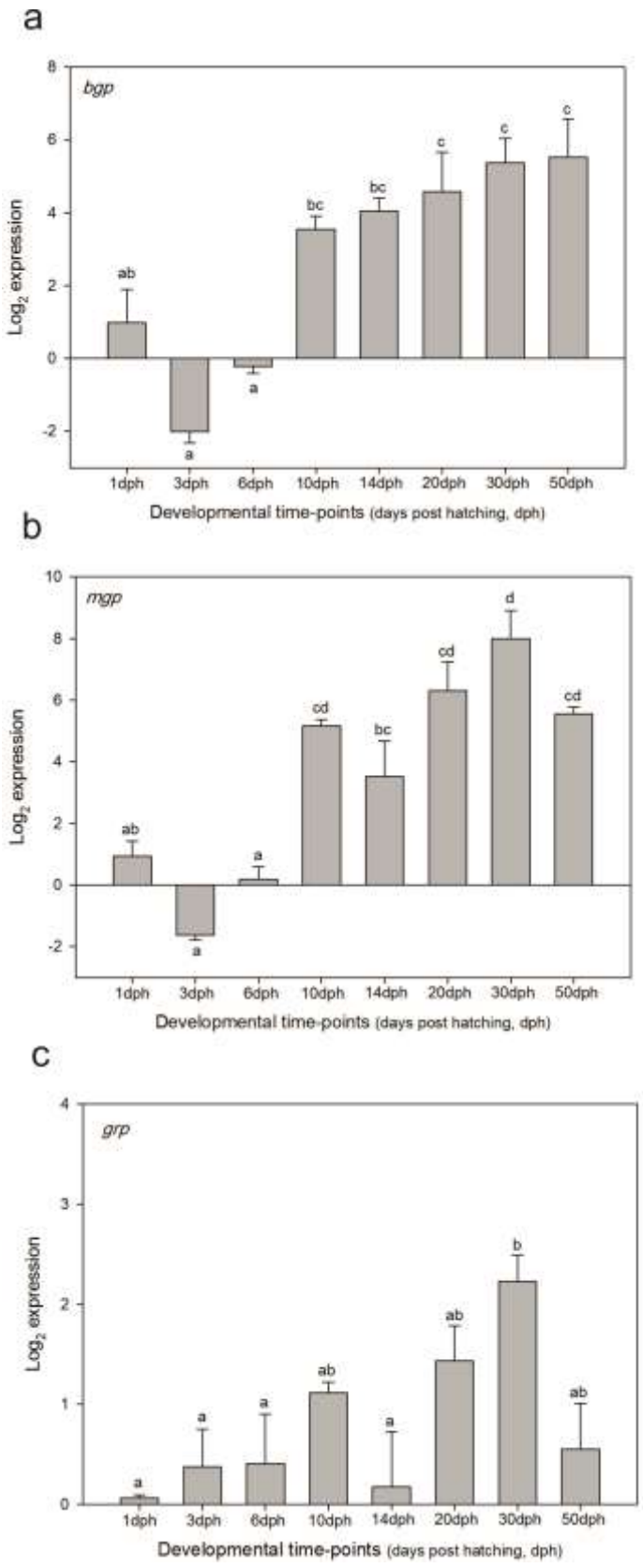


760

761

762

763

764